Supplementary material for Design and evaluation of a catalytic stripper with a plate electrical aerosol classifier

Chengxiang Guo[1,2], Tongzhu Yu[1,3*], Yixin Yang[1*], Huaqiao Gui[1,2,3], Zhe Ji[1,2,4], Jian Wang[3], Jianguo Liu[1,2,5], Wenqing Liu[1,2,3]

[1]Key Laboratory of Environmental Optics and Technology, Anhui Institute of Optics and Fine Mechanics, Hefei Institutes of Physical Science, Chinese Academy of Sciences, Hefei, 230031, China.

[2]University of Science and Technology of China, Hefei, 230026, China.

[3]Institute of Environmental Hefei Comprehensive National Science Center, Hefei, 231299, China.

[4]Key Laboratory of Vehicle Emission Control and Simulation of Ministry of Ecology and Environment, Chinese Research Academy of Environmental Sciences, Beijing 100012, China.

[5]University of Chinese Academy of Sciences, Beijing, 100049, China.

Correspondence to: Tongzhu Yu (tzyu@aiofm.ac.cn) and Yixin Yang (yxyang@aiofm.ac.cn)

Appendix A. Experimental setup

A.1. Removal efficiency of volatile particles

Figure S1 shows the experimental setup for the removal efficiency of CS for tetracontane. Line ① represents the removal efficiency of polydisperse tetracontane particles, and line ② represents the removal efficiency of monodisperse tetracontane.

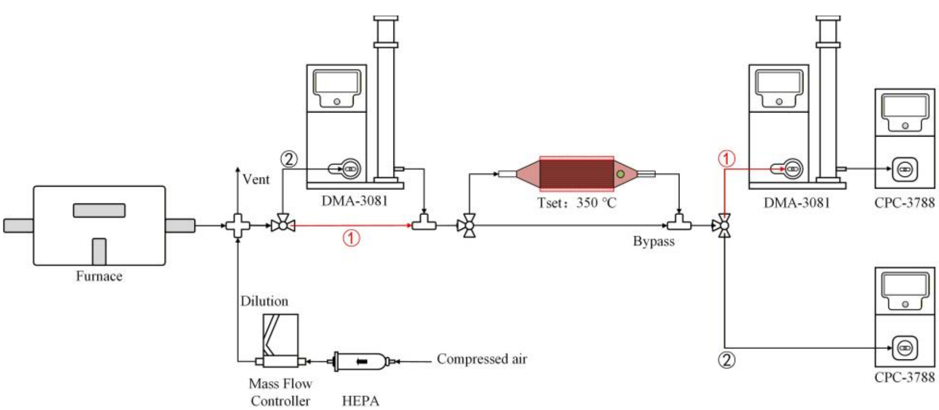

Figure S1: CS removal efficiency experiment setup.

Table S1

Experimental configurations for measuring the removal efficiency (RE) of tetracontane particles.

Material	Tetracontane
CS Temp (°C)	350
Particle size (nm)	30, 70, 100, 130, 150, 170, 200
$\boldsymbol{Q_{sa}}$ (L/min)	0.6, 1.5

A.2. Solid particle penetration experiments

Figure S2 shows the experimental setup for the particle penetration efficiency. The voltage of EAC set to 0. Classified soot particles are alternately introduced into the CS+EAC and bypass through valve control, and then measured to obtain N_{cs} and N_{bypass}. Under the condition that the concentration of classified particles remains stable, each measurement path is measured for two minutes. After eight alternating measurements, four penetration efficiencies are obtained using Eq. (17). The average of the four penetration efficiencies is the final penetration efficiency.

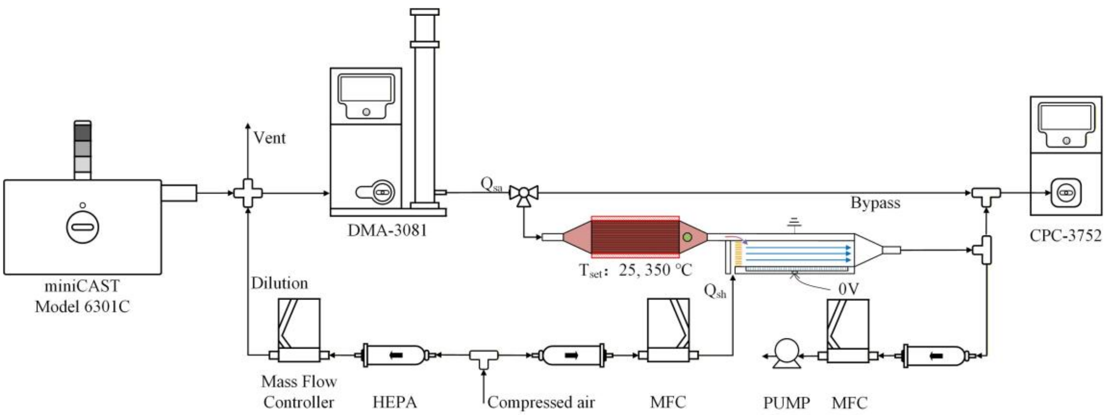

Figure S2: Solid particle penetration efficiency experiment setup.

Table S2

Experimental parameters for measuring particle penetration efficiency.

Experimental setup	CS+EAC
Material	Soot particle
CS Temp (°C)	25, 350
$\boldsymbol{Q_{sa}}$ (L/min)	0.3
Dilution ratio	1(undiluted), 2, 3, 4
EAC voltage (V)	The voltage was linearly regulated within 120 s, with the voltage range increasing proportionally to particle size.

A.3. Voltage-penetration efficiency curves for CS+EAC

Figure S3 shows the voltage-penetration efficiency curve experimental setup for CS+EAC. When the CS+EAC setup is set according to the red parameters, this setup is used for the 10 nm or 23 nm interval measurements in section 2.3.5.

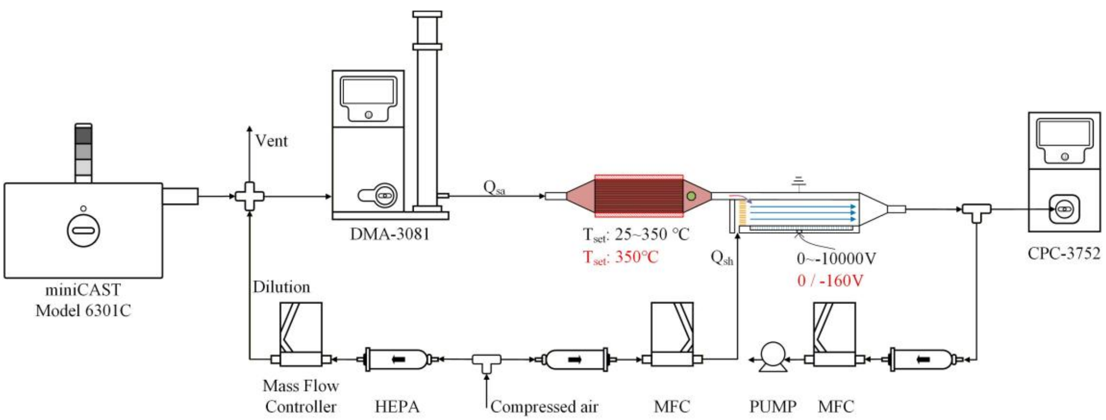

Figure S3: Voltage-penetration efficiency curve experiment setup for CS+EAC.

A.4. Measurement of particle size distribution at different voltages

Figure S4 shows the experimental setup for measuring the particle size distribution changes of polydisperse particles under different voltage settings in the CS+EAC. The polydisperse particles are alternately introduced into the bypass or CS+EAC after being charged by soft X-rays, and their particle size distribution is subsequently measured by the SMPS. In this setup, Q_{sa} is set to 0.3 L/min, Q_{sh} entering the EAC is 0.9 L/min, the sheath flow for the DMA is set to 3 L/min, and the inlet flow rate for the CPC is 0.3 L/min. To prevent uncharged neutral particles from being recharged in the SMPS, the soft X-ray charger in the SMPS is turned off.

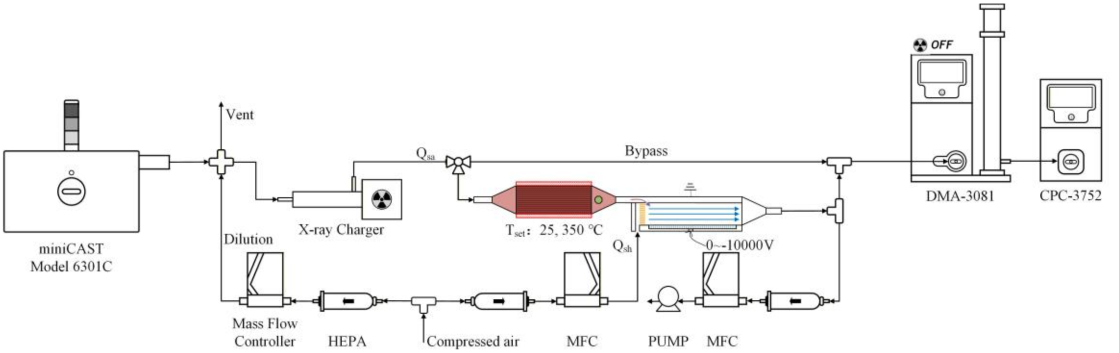

Figure S4: Voltage-particle size distribution experiment setup for CS+EAC.

Appendix B. Volatile particle removal efficiency

To evaluate compliance with regulatory standards, the RE tests were carried out on monodisperse and polydisperse tetracontane particles using the CS. Figure S5 presents the monodisperse tetracontane RE data for the CS heated to 350°C. The results indicate that the RE of the CS at sample flow rates of 0.6 and 1.5 L/min complies with Euro 6 regulations. However, RE declines as the size of tetracontane particles increases. Specifically, at 0.6 L/min, RE drops below 99.99% for 170 nm particles, while at 1.5 L/min, RE falls below 99.9% for 150 nm particles. In addition, the RE was higher at 0.6 L/min operation than at 1.5 L/min due to the longer particle residence time at 0.6 L/min.

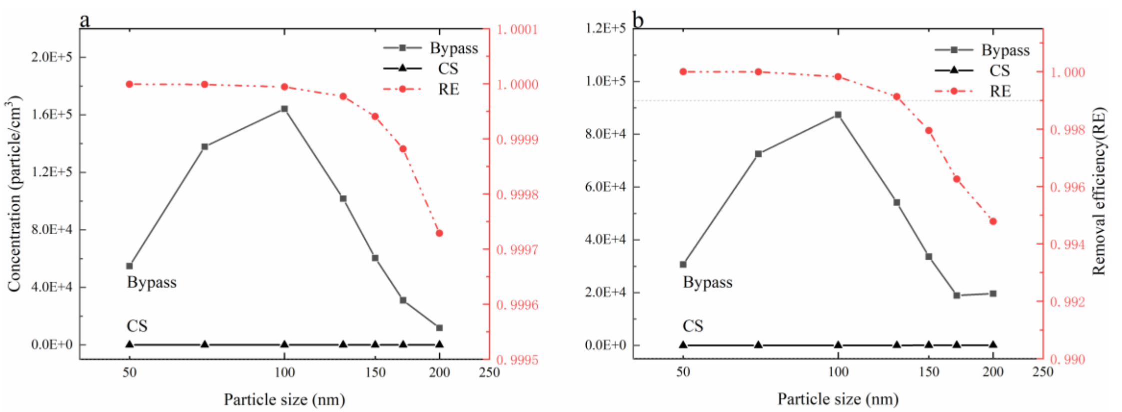

Fig. S5: Removal efficiency of monodisperse tetracontane particles at different sample flow rates: (a) 0.6 L/min, and (b) 1.5 L/min.

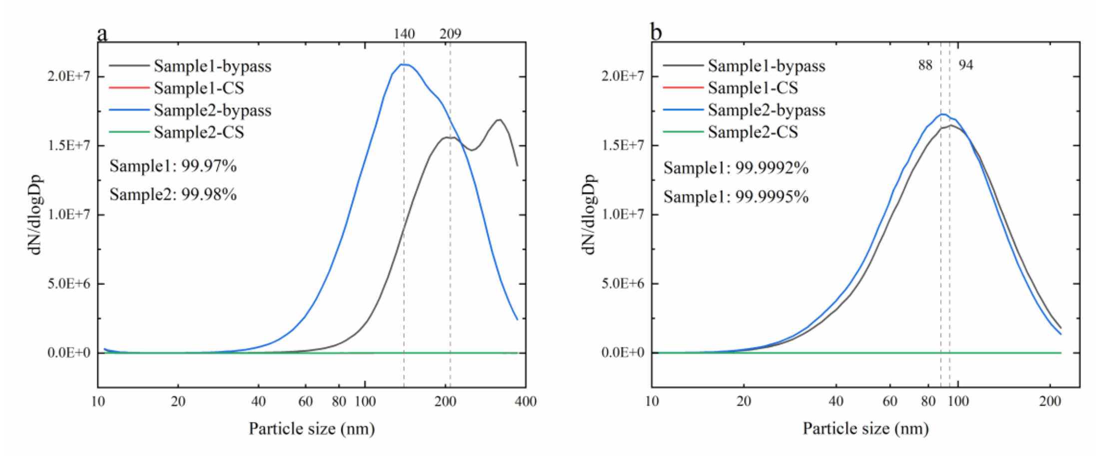

Fig. S6: Removal efficiency of polydisperse tetracontane particles at different sample flow rates: (a) 0.6 L/min, and (b) 1.5 L/min.

Table S3

Experimental data on the removal efficiency of volatile particles, including mass concentration and the corresponding removal efficiency.

Sample flow rates (L/min)	Sample number	CMD (nm)	Bypass (mg/m³)	CS (mg/m³)	Bypass (#/cm³)	CS (#/cm³)	RE (PM) (%)	RE (PN) (%)
0.6	1	140	47.8	8.5E-3	7.24E6	2191.9	99.982	99.97
	2	209	29	3.89E-3	1.04E7	1183.2	99.987	99.98
1.5	1	88	4.23	7.99E-6	7.57E6	59.85	99.9998	99.9992
	2	94	3.9	2.4E-5	7.9E6	40.03	99.9993	99.9995

To evaluate the CS performance with polydisperse tetracontane removal efficiency, experiments were carried out by adjusting the temperature of the tube furnace to generate tetracontane particles varying in median particle sizes and concentrations. The experimental results, presented in Fig. S6, demonstrated that the CS achieves removal efficiency meeting the Euro VII requirements at both sample flow rates. Specific mass concentration data can be found in Table S3. Although the median particle size of CS at 1.5 L/min is lower than that at 0.6 L/min, resulting in higher removal efficiency at the higher flow rate—the overall conclusion vindicates that the lower flow rate, the higher the removal efficiency.

Appendix C. CS+EAC voltage-penetration efficiency curve

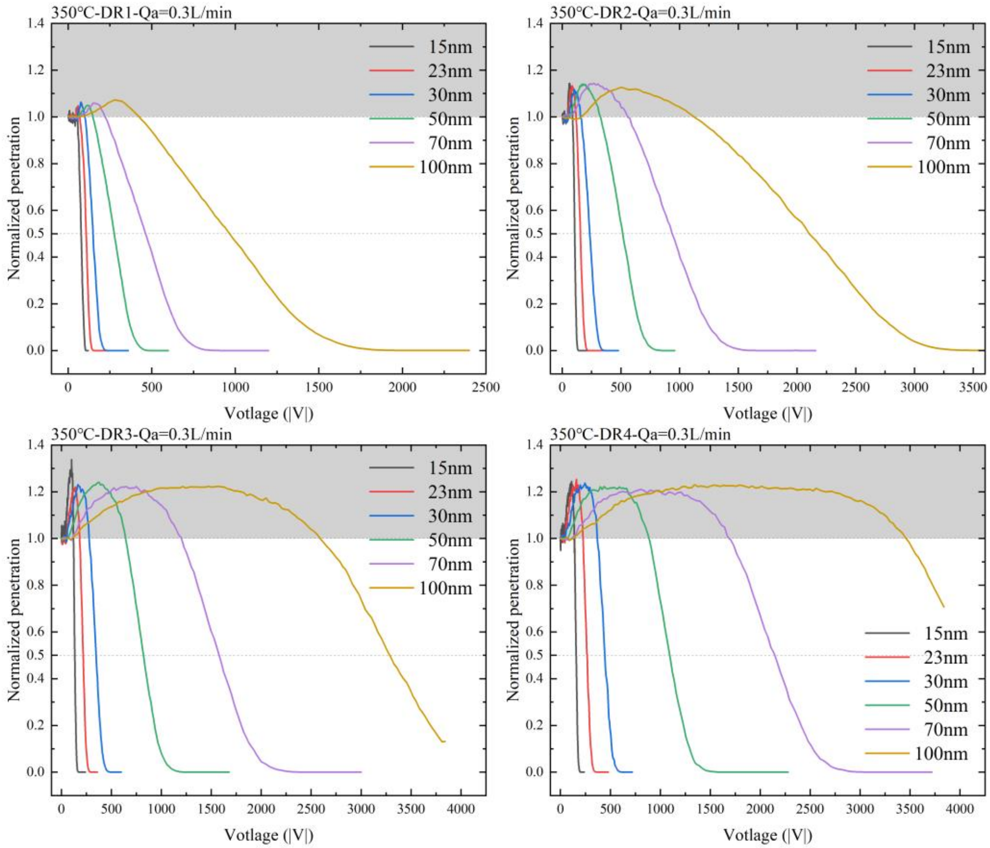

Fig. S7: CS+EAC voltage-penetration efficiency curves at varying temperatures.

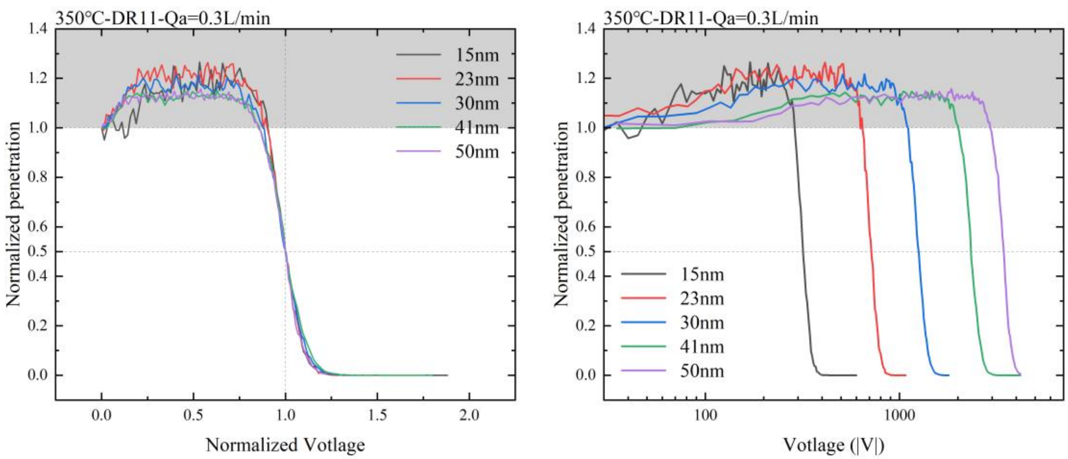

Fig. S8: Voltage-penetration efficiency curve at DR 11.

Appendix D. Regulatory requirements for volatile particle removers

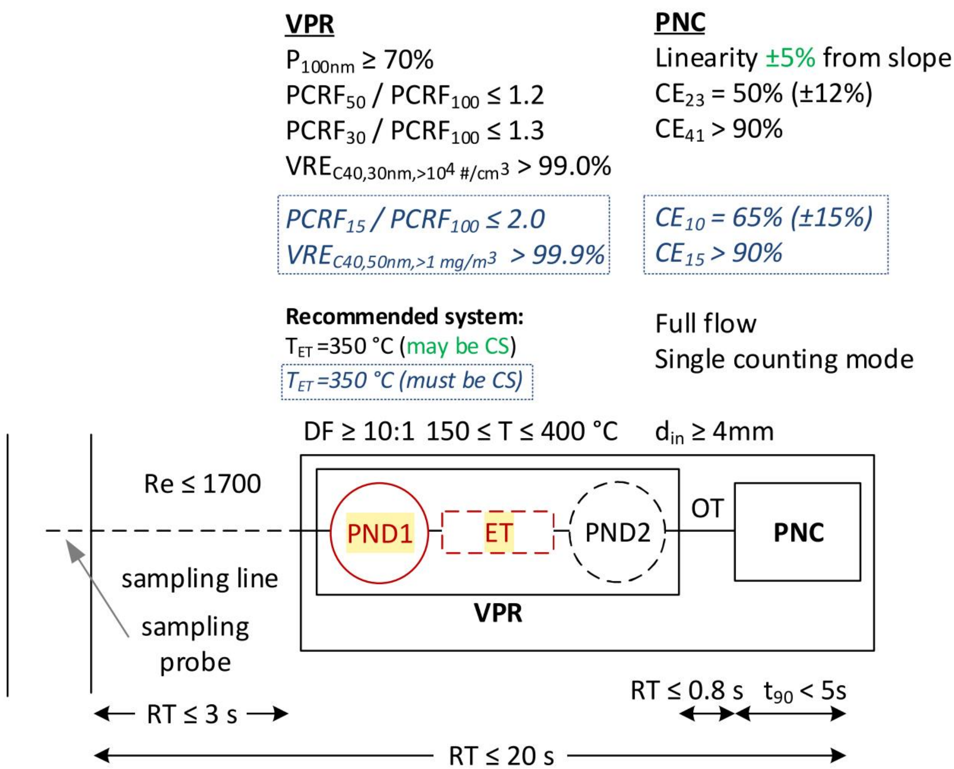

Figure S9: Schematic of a laboratory particle number system (LABS). Dashed lines show optional parts. In red are heated parts. At the top of the figure the calibration requirements are given. In green are the improvements compared to the original regulation (both counting >23 nm). The differences between 10-nm and 23-nm systems are given in blue italics and in dotted square. CE = counting efficiency; CS = catalytic stripper; DF = dilution factor; ET = evaporation tube; OT = outlet tube; P = penetration; PCRF = particle number concentration reduction factor; PNC = particle number counter; PND = particle number diluter; RT = residence time; t = time; T = temperature; VRE = volatile removal efficiency; VPR = volatile particle remover (Giechaskiel et al., 2021).

References

Giechaskiel, B., Melas, A., Martini, G., & Dilara, P.: Overview of vehicle exhaust particle number regulations. Processes, 9(12), 1–25, 2021. https://doi.org/10.3390/pr9122216